Geometric data analysis

Lecture 5/7 – Riemannian metrics and geodesics

Jean Feydy
HeKA team, Inria Paris, Inserm, Université Paris-Cité

Thursday, 9am–12pm – 7 lectures

Faculté de médecine, Hôpital Cochin, rooms 2001 + 2005

Validation: project + quizz

Recap of the previous lectures

To mitigate the **curse of dimensionality**, we use:

- **Expert** knowledge: high-quality features.
- Relevant **families** of functions: kernels, convolutional networks.
- Relevant **neighborhood** structures: graphs.

Main challenge: **local** implementation $\Longrightarrow$ **global** understanding.

Produce **guidelines** and **insights** for practitioners.

Large graphs are best understood as continuous objects [Pey11, EPW11]

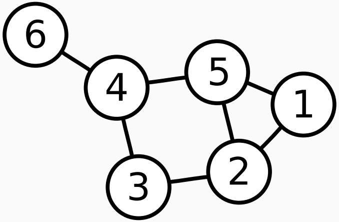

Simple graph.

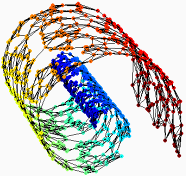

Manifold **hypothesis**.

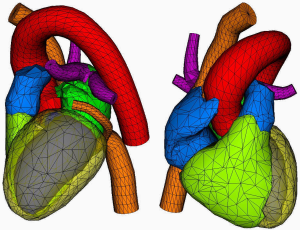

Physical manifold.

Long history in physics [Dat18, Bria, NWRC22]

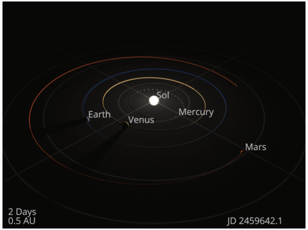

The **Solar** system.

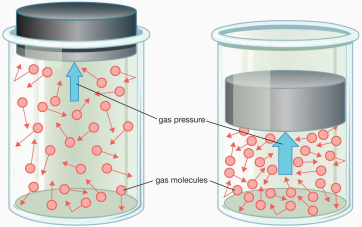

The **ideal gas** model.

Fluid simulation.

Remaining lectures

Lecture 5 – From discrete graphs to **continuous spaces**:

- The Poincaré disk.
- Local metrics and geodesics.

Lecture 6 – From discrete samples to **continuous distributions**:

- Duality: distributions and adversarial norms.
- Information geometry, kernels and optimal transport.

Lecture 7 – **Hardware** bottlenecks:

- Registers, parallel cores and compilers.
- Current trends.

References [Ghy06, CFK+97, Lee97, Fey20]

Textbooks and introductions – in English:

- *Poincaré and his disk* – Étienne Ghys, 2006.
- *Hyperbolic geometry* – Cannon et al., 1997.
- *Riemannian geometry: an introduction to curvature* – John M. Lee, 1997.
- *Geometric data analaysis, beyond convolutions* – my PhD thesis, 2020.

Lecture notes available on my website – in French:

- *Culture mathématique*.
- *Introduction à la géométrie riemannienne par l'étude des espaces de formes*.

The Poincaré disk

Science and hypothesis – Henri Poincaré, 1902

The Non-Euclidean World. – **If** geometrical space were a framework imposed on **each** of our representations considered **individually**, it would be **impossible** to represent to ourselves an image without this framework, and we should be quite **unable** to change our geometry.

But this is not the case; geometry is only the summary of the laws by which these images succeed each other.

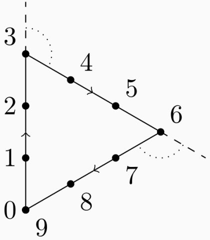

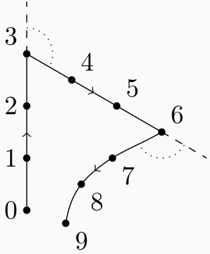

Science and hypothesis – Henri Poincaré, 1902

There is nothing, therefore, to prevent us from imagining a **series of representations**, similar in every way to our ordinary representations, but succeeding one another according to laws which **differ** from those to which we are accustomed.

We may thus conceive that beings whose education has taken place in a medium in which those laws would be so different, might have **a very different geometry** from ours.

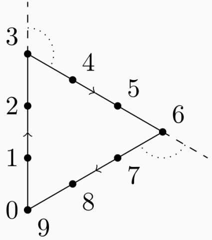

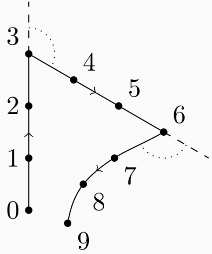

Suppose, for example, a world **enclosed in a large sphere** and subject to the following laws:

- The **temperature is not uniform;** it is **greatest at the centre**, and gradually decreases as we move towards the **circumference** of the sphere, where it is **absolute zero**.

  The **law of this temperature is as follows:** if R be the radius of the sphere, and r the distance of the point considered from the centre, the absolute temperature will be **proportional** to $R^2 - r^2$.

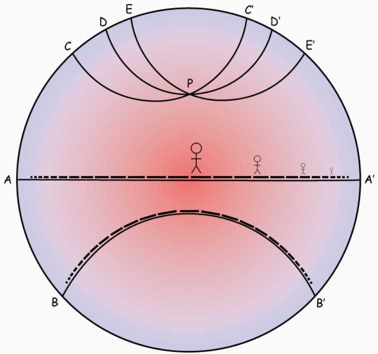

Science and hypothesis – Henri Poincaré, 1902 [Nor]

- Further, I shall suppose that in this world **all bodies have the same coefficient of dilatation**, so that the linear **dilatation** of any body is proportional to its absolute **temperature**.

- Finally, I shall assume that a body transported from one point to another of different tem- perature is **instantaneously** in thermal **equilibrium** with its new environment.

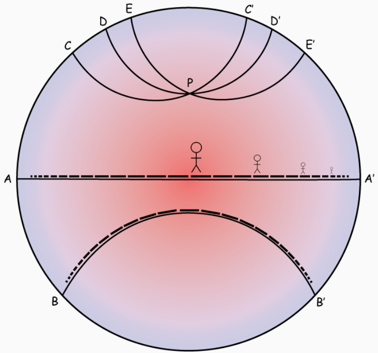

Science and hypothesis – Henri Poincaré, 1902 [Nor]

There is **nothing** in these hypotheses either **contradictory** or **unimaginable**. A moving object will become **smaller and smaller** as it approaches the **circumference** of the sphere.

Let us observe, in the first place, that although from the point of view of **our** ordinary geometry this world is **finite**, **to its inhabitants it will appear infinite**.

As they approach the surface of the sphere they become **colder**, and at the same time smaller and smaller. The steps they take are therefore also **smaller** and smaller, so that they can never reach the **boundary** of the sphere.

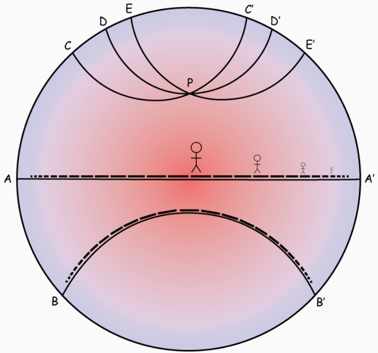

The Poincaré metric is locally a Euclidean metric

With $x^2 + y^2 < 1$, we define:

$$\mathrm{d}\Big((x,y) \to (x,y) + (\mathrm{d}x, \mathrm{d}y)\Big) \;=\; 2\,\frac{\sqrt{\mathrm{d}x^2 + \mathrm{d}y^2}}{1 - (x^2 + y^2)}$$

In other words:

$$\mathrm{d}^2\Big((x,y) \to (x,y) + (\mathrm{d}x, \mathrm{d}y)\Big) \;=\; 4\,\frac{\mathrm{d}x^2 + \mathrm{d}y^2}{\big(1 - (x^2 + y^2)\big)^2}$$

This **local** Euclidean metric is the **Riemannian** metric:

$$\|(\mathrm{d}x, \mathrm{d}y)\|^2_{(x,y)} \;=\; \big\langle\, (\mathrm{d}x, \mathrm{d}y)\,,\; g_{(x,y)}\,(\mathrm{d}x, \mathrm{d}y)\,\big\rangle$$

$$g_{(x,y)} \;=\; \begin{pmatrix} 4/\big(1 - (x^2 + y^2)\big)^2 & 0 \\ 0 & 4/\big(1 - (x^2 + y^2)\big)^2 \end{pmatrix}$$

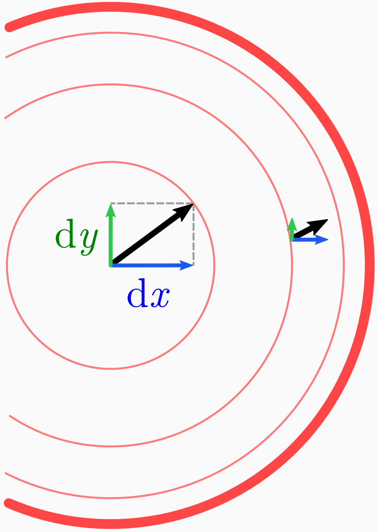

Length of curve

If $\gamma : [0,1] \to B(0,1)$ is a **smooth path**, we define:

$$\ell(\gamma) \;=\; \int_0^1 \|\dot\gamma(t)\|_{\gamma(t)}\,\mathrm{d}t$$

For the **straight path** $\gamma(t) = (t,0)$, we find:

$$\begin{aligned}\ell(\gamma) \;&=\; \int_0^1 \|(1,0)\|_{(t,0)}\,\mathrm{d}t \\ &=\; \int_0^1 \frac{2}{1-t^2}\,\mathrm{d}t \\ &=\; \int_0^1 \frac{2}{(1+t)(1-t)}\,\mathrm{d}t \;=\; +\infty\end{aligned}$$

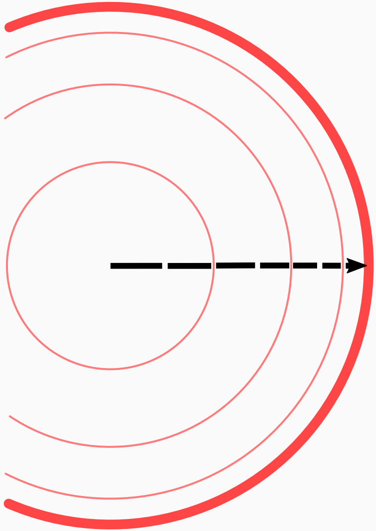

The Poincaré disk is **a universe in a nutshell**.

Tissot's indicatrix [Brib, Kü04]

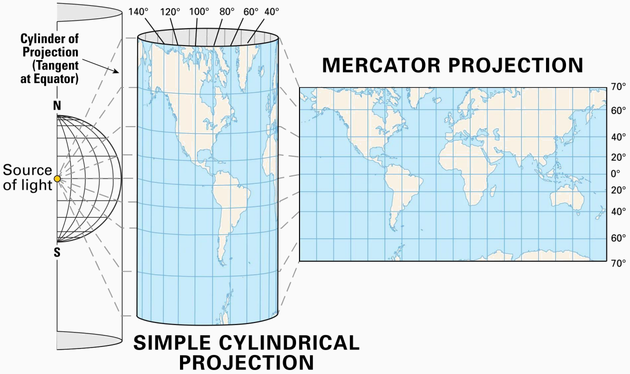

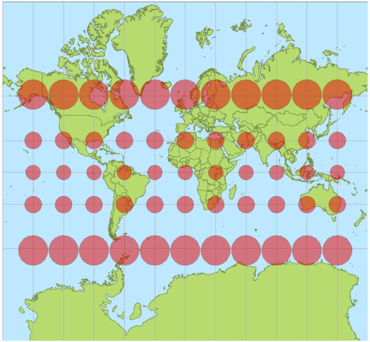

Tissot's indicatrix at location (x, y) is a **unit ball** for the local metric.

This ellipsoid allows us to **depict distortions** in cartography

and fully describes a **Riemannian metric** on the 2D map.

Equivalent descriptions of the Poincaré segment $(-1, +1)$

Stereographic projections define bijections between
the segment I, the half-circle J and the half-line H.

If we endow I with the Poincaré metric:

$$\|(\mathrm{d}x)\|_{(x)\in I} = 2\,\frac{\sqrt{\mathrm{d}x^2}}{1-x^2}\,,$$

then J and H are endowed with:

$$\|(\mathrm{d}x,\mathrm{d}z)\|_{(x,z)\in J} = \frac{\sqrt{\mathrm{d}x^2+\mathrm{d}z^2}}{z}$$

$$\|(\mathrm{d}z)\|_{(z)\in H} = \frac{\sqrt{\mathrm{d}z^2}}{z}$$

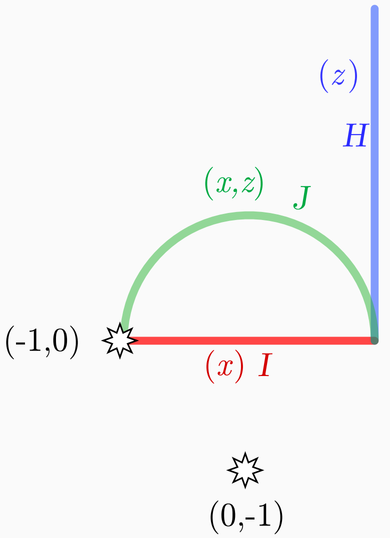

Equivalent descriptions of the Poincaré segment $(-1, +1)$

Stereographic projections define bijections between the segment I, the half-circle J and the half-line H.

If we endow I with the Poincaré metric:

$$\|(\mathrm{d}x)\|_{(x)\in I} = 2\,\frac{\sqrt{\mathrm{d}x^2}}{1-x^2}\,,$$

then J and H are endowed with:

$$\|(\mathrm{d}x, \mathrm{d}z)\|_{(x,z)\in J} = \frac{\sqrt{\mathrm{d}x^2 + \mathrm{d}z^2}}{z}$$

$$\|(\mathrm{d}z)\|_{(z)\in H} = \frac{\sqrt{\mathrm{d}z^2}}{z}$$

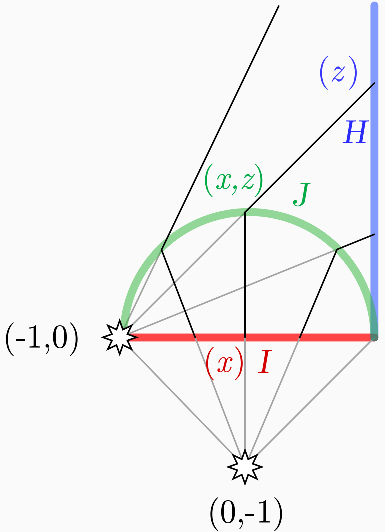

Equivalent descriptions of the Poincaré segment $(-1, +1)$

Stereographic projections define bijections between
the segment I, the half-circle J and the half-line H.

If we endow I with the Poincaré metric:

$$\|(\mathrm{d}x)\|_{(x)\in I} = 2\,\frac{\sqrt{\mathrm{d}x^2}}{1-x^2}\,,$$

then J and H are endowed with:

$$\|(\mathrm{d}x,\mathrm{d}z)\|_{(x,z)\in J} = \frac{\sqrt{\mathrm{d}x^2+\mathrm{d}z^2}}{z}$$

$$\|(\mathrm{d}z)\|_{(z)\in H} = \frac{\sqrt{\mathrm{d}z^2}}{z}$$

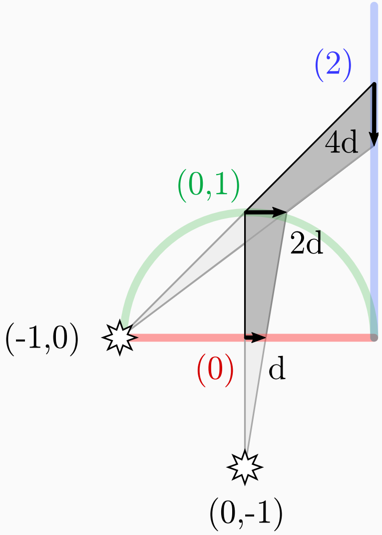

Equivalent descriptions of the Poincaré segment $(-1, +1)$

Stereographic projections define bijections between the segment I, the half-circle J and the half-line H.

If we endow I with the Poincaré metric:

$$\|(\mathrm{d}x)\|_{(x)\in I} = 2\,\frac{\sqrt{\mathrm{d}x^2}}{1-x^2}\,,$$

then J and H are endowed with:

$$\|(\mathrm{d}x,\mathrm{d}z)\|_{(x,z)\in J} = \frac{\sqrt{\mathrm{d}x^2+\mathrm{d}z^2}}{z}$$

$$\|(\mathrm{d}z)\|_{(z)\in H} = \frac{\sqrt{\mathrm{d}z^2}}{z}$$

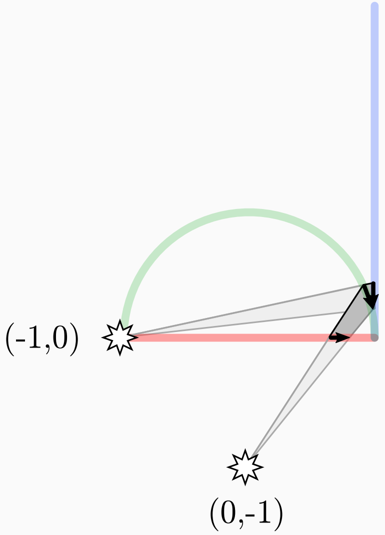

Equivalent descriptions of the Poincaré segment $(-1, +1)$

Stereographic projections define bijections between
the segment I, the half-circle J and the half-line H.

If we endow I with the Poincaré metric:

$$\|(\mathrm{d}x)\|_{(x)\in I} = 2\,\frac{\sqrt{\mathrm{d}x^2}}{1-x^2},$$

then J and H are endowed with:

$$\|(\mathrm{d}x, \mathrm{d}z)\|_{(x,z)\in J} = \frac{\sqrt{\mathrm{d}x^2 + \mathrm{d}z^2}}{z}$$

$$\|(\mathrm{d}z)\|_{(z)\in H} = \frac{\sqrt{\mathrm{d}z^2}}{z}$$

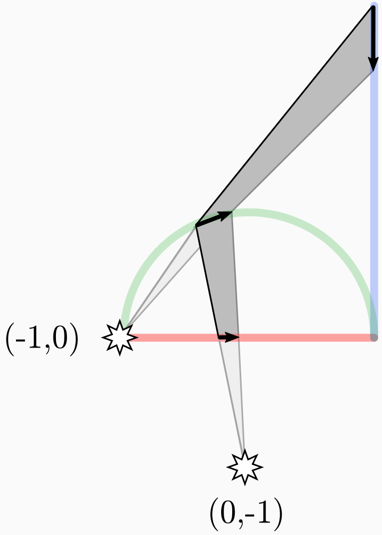

Equivalent descriptions of the Poincaré disk

Stereographic projections define bijections between
the disk I, the hemisphere J and the half-plane H.

If we endow I with the Poincaré metric:

$$\|(\mathrm{d}x, \mathrm{d}y)\|_{(x,y)\in I} = 2\,\frac{\sqrt{\mathrm{d}x^2 + \mathrm{d}y^2}}{1-(x^2+y^2)},$$

then J and H are endowed with:

$$\|(\mathrm{d}x, \mathrm{d}y, \mathrm{d}z)\|_{(x,y,z)\in J} = \frac{\sqrt{\mathrm{d}x^2 + \mathrm{d}y^2 + \mathrm{d}z^2}}{z}$$

$$\|(\mathrm{d}y, \mathrm{d}z)\|_{(y,z)\in H} = \frac{\sqrt{\mathrm{d}y^2 + \mathrm{d}z^2}}{z}$$

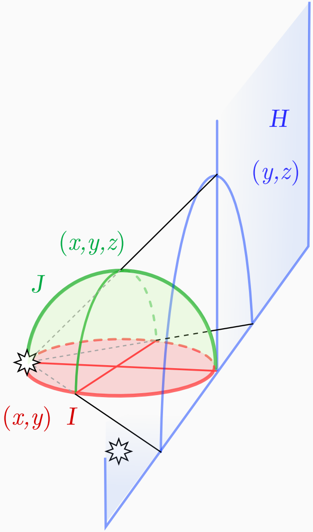

Tissot's indicatrix on the Poincaré disk, hemisphere and half-plane

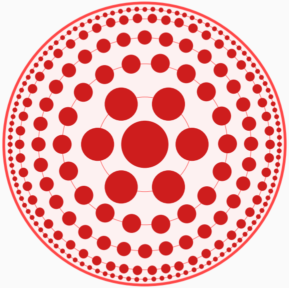

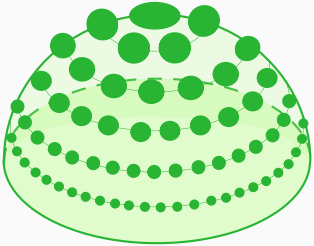

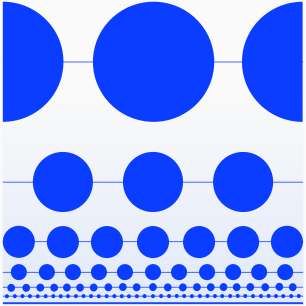

$$2\,\frac{\sqrt{\mathrm{d}x^2+\mathrm{d}y^2}}{1-(x^2+y^2)}$$

$$\frac{\sqrt{\mathrm{d}x^2+\mathrm{d}y^2+\mathrm{d}z^2}}{z}$$

$$\frac{\sqrt{\mathrm{d}y^2+\mathrm{d}z^2}}{z}$$

The discrete Poincaré grid

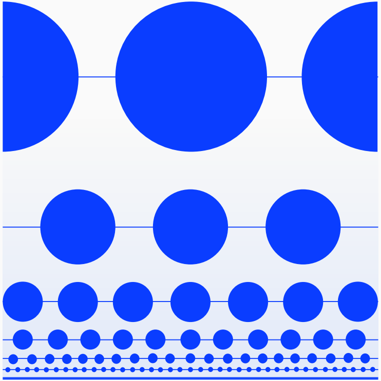

$$\frac{\sqrt{\mathrm{d}y^2 + \mathrm{d}z^2}}{z}$$

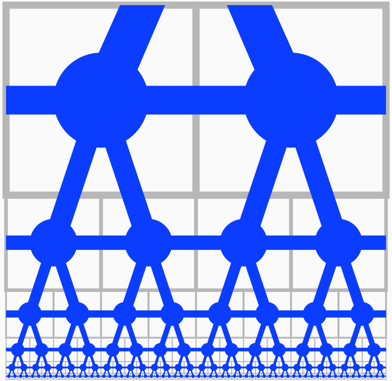

Octave grid based on a dyadic tree.

Geodesics on the Poincaré disk

Geodesics on the Poincaré grid

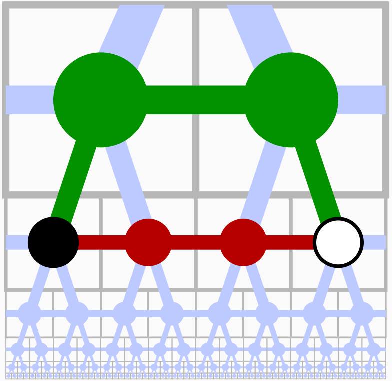

The green and red paths
have the same length.

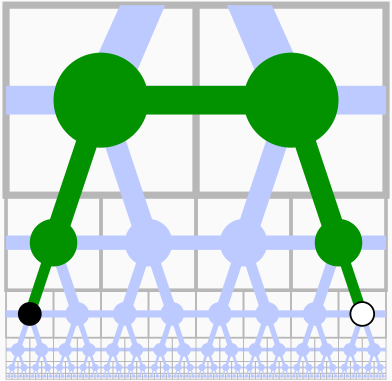

Going **up** is faster than
travelling **sideways**.

Vertical geodesics on the Poincaré half-plane

If the source and target points belong to the **vertical axis** $y = 0$, the shortest path is **straight**:

$$\begin{aligned} \ell(y(t), z(t)) &= \int_0^1 \frac{\sqrt{\dot{y}(t)^2 + \dot{z}(t)^2}}{z(t)} \mathrm{d}t \\ &\leqslant \int_0^1 \frac{\sqrt{\dot{z}(t)^2}}{z(t)} \mathrm{d}t \\ &= \ell(0, z(t)) \,. \end{aligned}$$

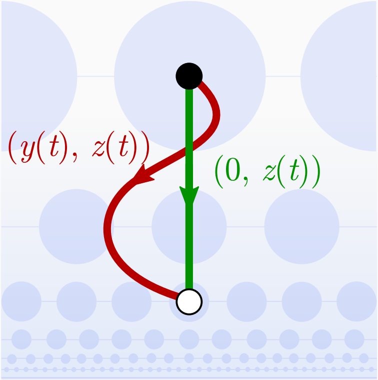

Centers of the three Poincaré models

Using our stereographic projections, the North pole $(x, y, z) = (0, 0, +1)$ of the **hemisphere** corresponds to:

- the center $(x, y) = (0, 0)$ of the **disk**,
- the point $(y, z) = (0, +2)$ of the **half-plane**.

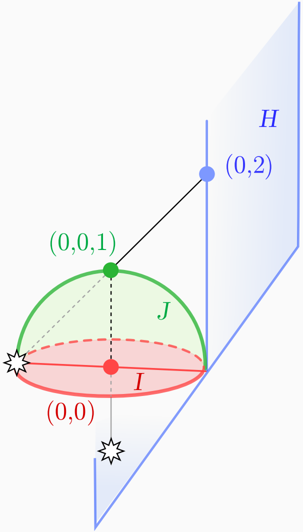

Geodesics on the Poincaré hemisphere

The vertical axis in the **half-plane** is equivalent to the **“Greenwich meridian”** in the **hemisphere**.

Since the Poincaré metric:

$$\|(\mathrm{d}x, \mathrm{d}y, \mathrm{d}z)\|_{(x,y,z)\in J} = \frac{\sqrt{\mathrm{d}x^2 + \mathrm{d}y^2 + \mathrm{d}z^2}}{z}$$

is invariant by **rotations**:

$$(x, y, z) \mapsto (\cos(\theta)\, x, \sin(\theta)\, y, z)\ ,$$

all great circles that pass through the North pole are also **geodesic curves**.

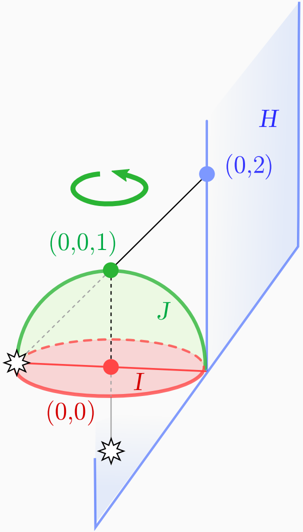

Geodesics on the Poincaré hemisphere

The vertical axis in the **half-plane** is equivalent to the **“Greenwich meridian”** in the **hemisphere**.

Since the Poincaré metric:

$$\|(\mathrm{d}x, \mathrm{d}y, \mathrm{d}z)\|_{(x,y,z)\in J} = \frac{\sqrt{\mathrm{d}x^2 + \mathrm{d}y^2 + \mathrm{d}z^2}}{z}$$

is invariant by **rotations**:

$$(x, y, z) \mapsto (\cos(\theta)\, x, \sin(\theta)\, y, z)\ ,$$

all great circles that pass through the North pole are also **geodesic curves**.

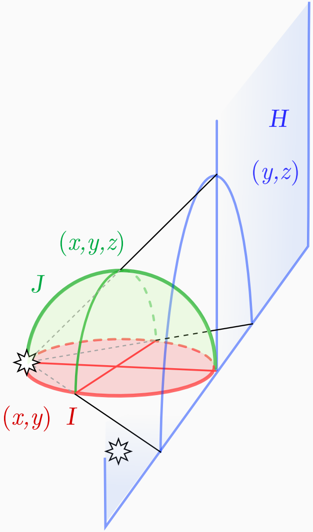

Meridians on the three Poincaré models

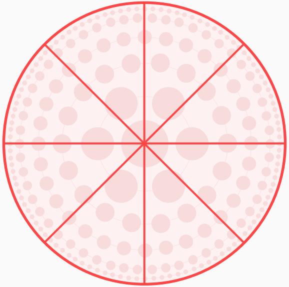

Diameters.

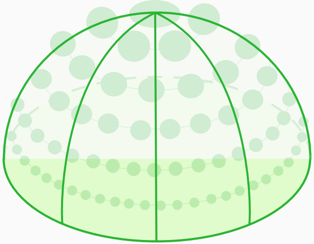

Meridians.

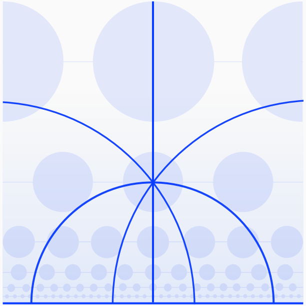

Half-circles that pass through $(y, z) = (0, +2)$.

Geodesics on the Poincaré half-plane

Half-circles that are perpendicular to the horizontal axis **are all geodesics**.

This is because the Poincaré metric:

$$\|(\mathrm{d}y, \mathrm{d}z)\|_{(y,z)\in H} = \frac{\sqrt{\mathrm{d}y^2 + \mathrm{d}z^2}}{z}$$

is invariant by **horizontal translations**:

$$(y, z) \mapsto (y + \Delta y, z)$$

and **scalings** with a positive constant $a > 0$:

$$(y, z) \mapsto (ay, az) \, .$$

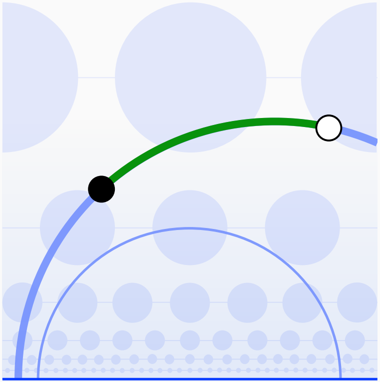

Geodesics on the Poincaré grid, half-plane and disk

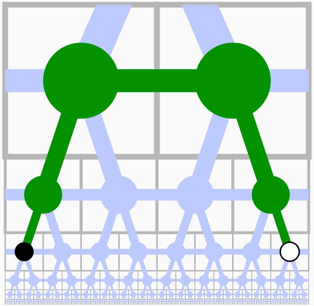

Up-and-down paths.

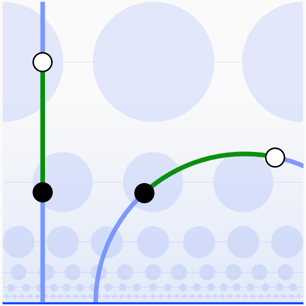

Half-circles and vertical lines.

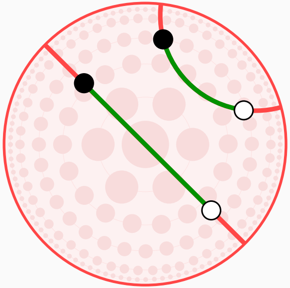

Orthogonal circles and diameters.

A continuous tree

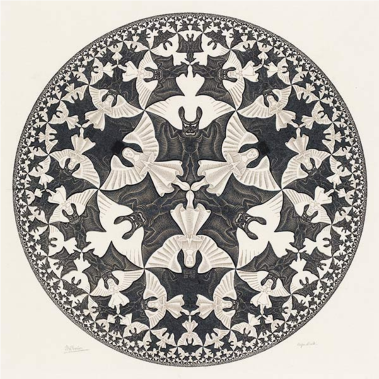

Circle Limit IV by **M.C. Escher**:
a **regular** tiling of the Poincaré disk.

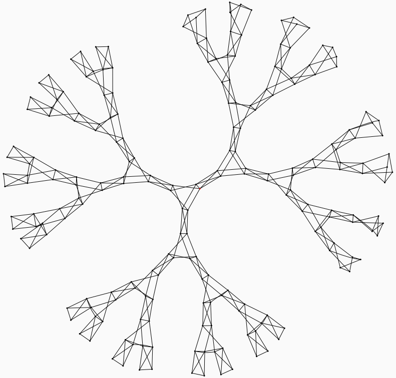

The Cayley graph of $SL_2(\mathbb{Z})$
is to the **Poincaré** disk what a
regular grid is to the **Euclidean** plane.

Recap on the Poincaré disk

We should **remember** that:

- A **Riemannian** metric is a smooth field of Euclidean norms.
  It is equivalent to **Tissot's indicatrix** in cartography.
- **Convenient** way of defining arbitrary geometries:
  the Poincaré disk is a continuous tree.
- **Changes of coordinates** are key to eloquent proofs.
  Don't get stuck on one parameterization.
- **Discrete** $\leftrightarrow$ **Continuous** analogies go both ways.

Riemannian geometry, in practice

A convenient way of working with surfaces

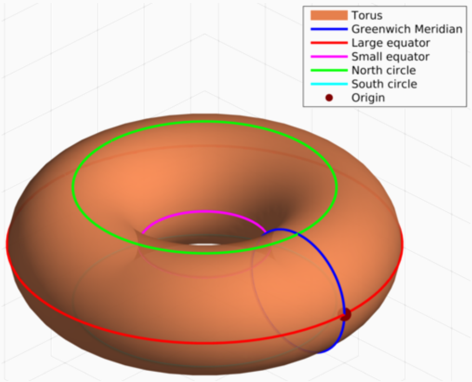

As a surface **embedded in 3D**.

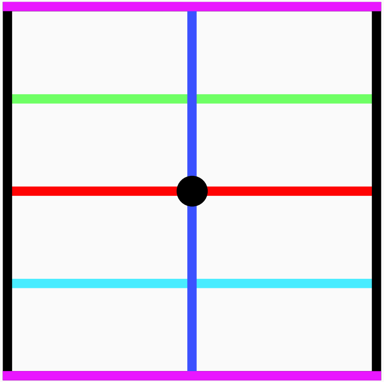

The torus as a **flat 2D square**.

A convenient way of working with surfaces

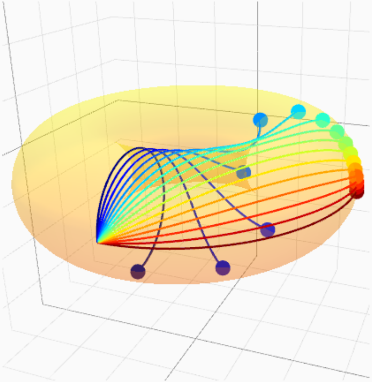

Geodesics on the donut.

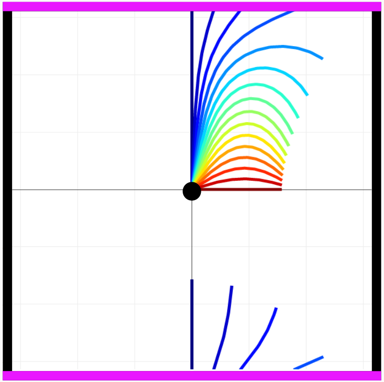

The torus as a **curved 2D square**.

Mathematical objects [AFPA06, KSA19]

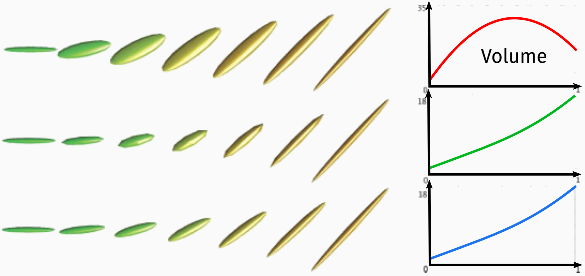

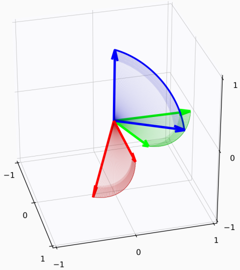

Covariance matrices: geodesics for the Euclidean, affine-invariant and log-Euclidean metrics.

3D rotations: geodesics for the Lie group structure.

Probability distributions – see Lecture 6! [PC18]

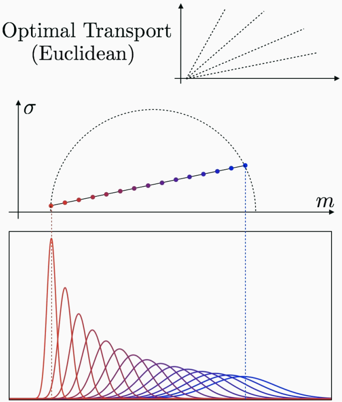

Gaussians + **Wasserstein** metric

= **Euclidean**.

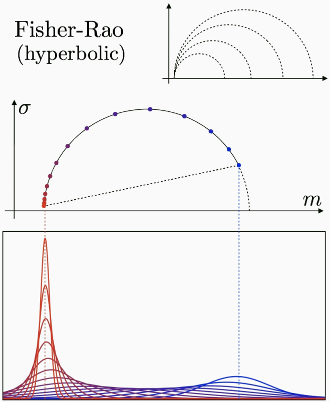

Gaussians + relative **entropy**

= **Poincaré**.

Shape metrics – remember Lecture 1!

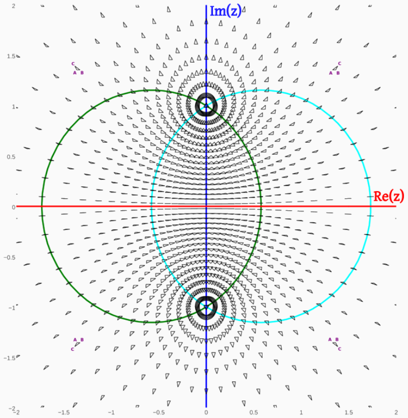

The **plane** of triangle shapes.

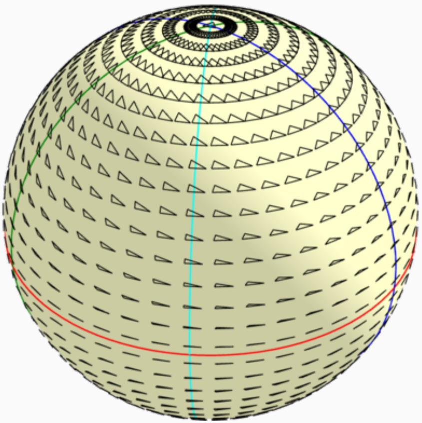

The **sphere** of triangle shapes.

Shape metrics [KMP07]

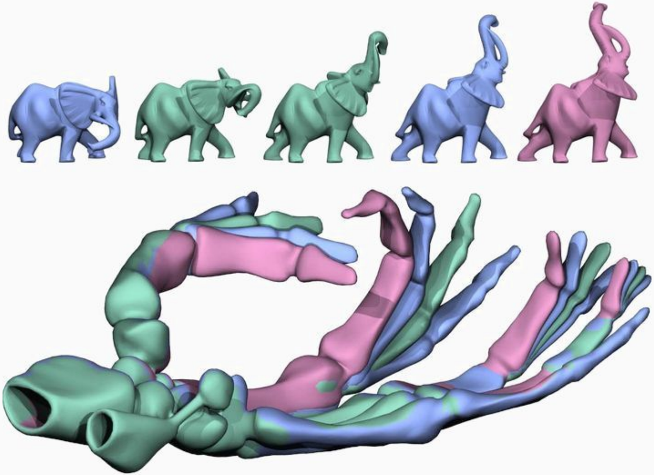

Geodesics in spaces of elephants and skeletons.

Shape metrics [vRESH16]

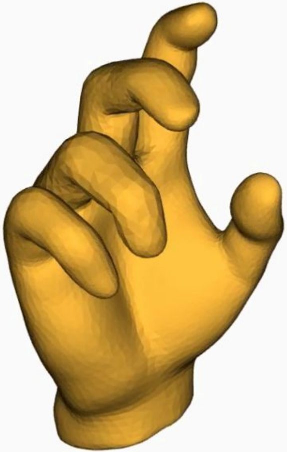

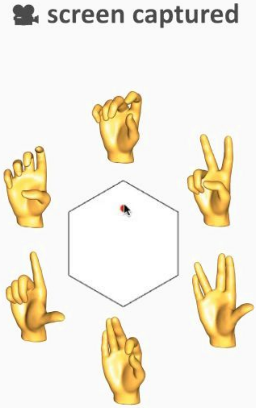

Barycentric interpolation in a space of hands.

Network architectures are “projections” from parameter space to function space

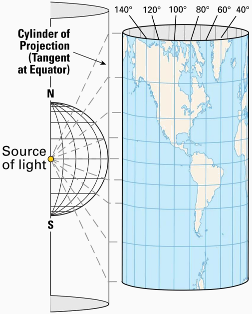

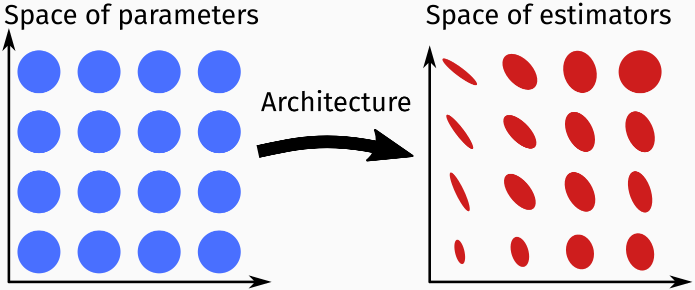

Standard gradient descent on the parameters

$\Longleftrightarrow$ **Riemannian** gradient descent on the network.

Core idea behind the **natural gradient**, neural **tangent kernels**,

(Wasserstein) **gradient flows**…

Graph and point cloud embeddings [SDSGR18, NK17]

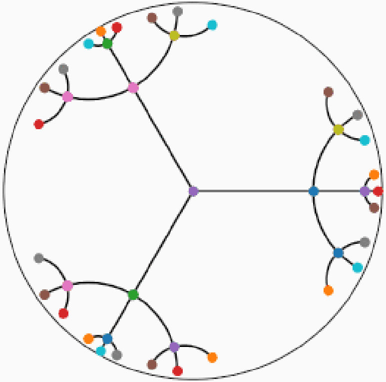

Embedding a **tree** in the Poincaré disk.

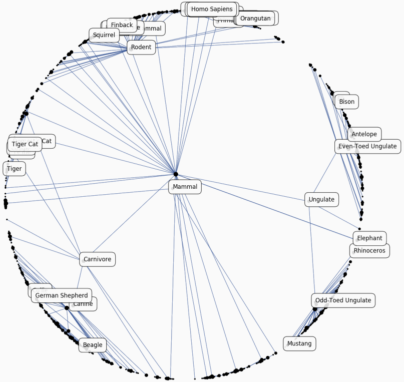

WordNet **mammals** subtree

UMAP (Uniform **Manifold** Approximation and Projections)
also works with Riemannian metrics.

The geodesic equation – Hamiltonian form

If $H(q,p) = \frac{1}{2}\langle\, p\,,\, g_q^{-1} p\,\rangle$ denotes the **Hamiltonian** for the Riemannian metric g_q, we can show that **paths** $q(t)$ that **minimize length** locally and travel at **constant speed** follow a **coupled Ordinary Differential Equation** with a **momentum** vector $p(t)$:

$$\begin{cases} \dot{q}(t) \;=\; +\,\frac{\partial H}{\partial p}(q(t), p(t)) \\ \dot{p}(t) \;=\; -\,\frac{\partial H}{\partial q}(q(t), p(t)) \end{cases}$$

follow the velocity $v(t) = g_{q(t)}^{-1} p(t)$.

steer the momentum to stay on a geodesic path.

Geodesic paths are fully determined by:

- the starting **position** $q(t=0)$,
- the starting **momentum** $p(t=0) \iff$ the **velocity** $\dot{q}(t=0) = g_{q(t=0)} p(t=0)$.

The exponential map [Chr10, Rok08]

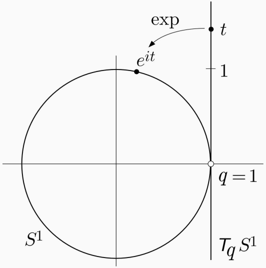

From the 1D line to the **circle**.

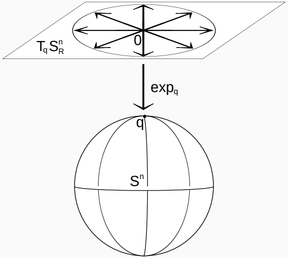

From the 2D plane to the **sphere**.

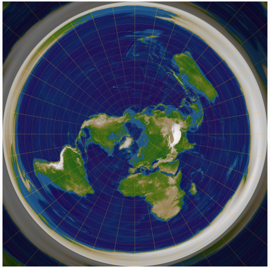

Azimuthal equidistant projection.

$\exp_{q_0}(p_0)$ denotes the **solution** $q(t=1)$ of the geodesic equation with **initial condition** $q(t=0)=q_0, p(t=0)=p_0$.

Computing geodesics from A to B – three main scenarios

1. The metric has a lot of structure – closed formulas:

- Just like the Poincaré disk: simple example + symmetries.
- Riemannian **metric** $\iff$ Relevant **kernel**.

2. The metric g_x is simple – path shortening:

- Discretize the path energy $\ell^2(\gamma) \simeq \frac{1}{\mathsf{N}} \sum_{i=1}^{\mathsf{N}} \mathsf{N}^2 \, \|\gamma(i/\mathsf{N}) - \gamma((i-1)/\mathsf{N})\|^2_{\gamma(i/\mathsf{N})}$.
- "Mean curvature flow": gradient descent with respect to the snapshot positions.

3. The cometric $K_q = (g_q)^{-1}$ is simple – geodesic shooting:

- **Implement** the exponential $(q_0, p_0) \mapsto \exp_{q_0}(p_0)$ by integrating the Hamilton ODE.
- **Solve** the inverse problem $p_0 \mapsto \exp_A(p_0) \simeq B$ with an optimizer or a network.

Conclusion

Riemannian metrics provide:

- Expressive **vocabulary**: trees, balls, shapes and probability distributions.
- Complete **toolbox**: local metric $\longrightarrow$ geodesics, exponentials and barycenters.
- Appealing **message**:

simple paths on a curved space $>$ **complex paths on a flat space.**

This framework is the cornerstone of several applied fields,
and provides an **inspiring** outlook in many other settings.

$\Longrightarrow$ **Lab session** with GeomStats. $\Longleftarrow$

References

References i

Vincent Arsigny, Pierre Fillard, Xavier Pennec, and Nicholas Ayache.

Log-euclidean metrics for fast and simple calculus on diffusion tensors.

Magnetic Resonance in Medicine: An Official Journal of the International Society for Magnetic Resonance in Medicine, 56(2):411–421, 2006.

Encyclopædia Britannica.

Ideal gas.

https://www.britannica.com/science/ideal-gas.

References ii

Encyclopædia Britannica.

Mercator projection.

https://www.britannica.com/science/Mercator-projection.

James W Cannon, William J Floyd, Richard Kenyon, Walter R Parry, et al.

Hyperbolic geometry.

Flavors of geometry, 31(59-115):2, 1997.

- Christian1985.

  Exponential mapping from the tangent space to the sphere.

  https://fr.wikipedia.org/wiki/Fichier:Exponential_map_of_the_sphere.svg, 2010.

  CC BY-SA 3.0.

- Datumizer.

  Solar system orrery inner planets.

  https://commons.wikimedia.org/wiki/File:Solar_system_orrery_inner_planets.gif, 2018.

  CC BY-SA 4.0.

References iv

Olivier Ecabert, Jochen Peters, and Matthew Walker.

Segmentation of the heart and great vessels in ct images using a model-based adaptation framework.

Medical Image Analysis, (15):863–876, 2011.

Jean Feydy.

***Geometric data analysis, beyond convolutions*.**

PhD thesis, Université Paris-Saclay, 2020.

Étienne Ghys.

Poincaré and his disk.

The scientific legacy of Poincaré, 36:17, 2006.

Martin Kilian, Niloy J Mitra, and Helmut Pottmann.

Geometric modeling in shape space.

In *ACM Transactions on Graphics (TOG)*, volume 26, page 64. ACM, 2007.

References vi

Line Kühnel, Stefan Sommer, and Alexis Arnaudon.

Differential geometry and stochastic dynamics with deep learning numerics.

Applied Mathematics and Computation, 356:411–437, 2019.

Stefan Kühn.

Mercator projection map with tissot's indicatrices.

https://commons.wikimedia.org/wiki/File:Tissot_mercator.png, 2004.

CC BY-SA 3.0.

John M Lee.

Riemannian geometry: An introduction to curvature.

Graduate Texts in Mathematics, 176, 1997.

Maximillian Nickel and Douwe Kiela.

Poincaré embeddings for learning hierarchical representations.

Advances in neural information processing systems, 30, 2017.

John D. Norton.

Poincaré disk.

https://sites.pitt.edu/ jdnorton/jdnorton.html.

Mohammad Sina Nabizadeh, Stephanie Wang, Ravi Ramamoorthi, and Albert Chern.

Covector fluids.

ACM Transactions on Graphics (TOG), 41(4):113:1–113:15, 2022.

Gabriel Peyré and Marco Cuturi.

Computational optimal transport.

arXiv preprint arXiv:1803.00567, 2018.

Gabriel Peyré.

The numerical tours of signal processing-advanced computational signal and image processing.

IEEE Computing in Science and Engineering, 13(4):94–97, 2011.

RokerHRO.

Polar azimuthal equidistant projection of the earth (centered to north pole).

https://commons.wikimedia.org/wiki/File:Azimuthal_Equidistant_N90.jpg, 2008.

CC BY-SA 3.0.

Frederic Sala, Chris De Sa, Albert Gu, and Christopher Ré.

Representation tradeoffs for hyperbolic embeddings.

In *International conference on machine learning*, pages 4460–4469. PMLR, 2018.

Philipp von Radziewsky, Elmar Eisemann, Hans-Peter Seidel, and Klaus Hildebrandt.

Optimized subspaces for deformation-based modeling and shape interpolation.

Computers & Graphics, 58:128–138, 2016.